DOI 10.1007/s11094-023-02953-7
Pharmaceutical Chemistry Journal, Vol. 57, No. 6, September, 2023 (Russian Original Vol. 57, No. 6, June, 2023)

INTRANASAL MIRNAS-17/20 ADMINISTRATION ALLEVIATES EARLY BRAIN INJURY AFTER SUBARACHNOID HEMORRHAGE IN RATS

Ü. A. Malçok,[1,*] O. Doğanlar,[2] N. K. Tüfekçioğlu,[3] M. A. Ovalı,[3] D. Aykora,[3] Z. B. Doğanlar,[2] B. Büyük,[4] and M. Uzun[3]

Original article submitted May 27, 2022.

Early brain injury (EBI) in the first 24–72 h is the leading cause of mortality and disability related to subarachnoid hemorrhage (SAH). Both melatonin and microRNAs (miRs) are involved in the regulation of a number of neuronal molecular signaling procedures in the central nervous system, ranging from hypoxia, inflammation to neuronal apoptosis. The present study was performed to explore the effect of miRs-17/20 and combined treatment with melatonin on early brain injury after SAH and underlying molecular mechanisms in rats. In this study 54 Wistar albino rats were divided into six experimental groups: Sham, SAH, SAH + Melatonin, SAH+miRs-17/20 control, SAH+MEL+miRs-17/20, and SAH+MEL+miRs-17/20. The Garcia's Neurological Scoring Scale and motor coordination tests were used for clinical observation. H&E staining was performed to evaluate pathological score. The gene expression levels were determined by qRT-PCR and key proteins were quantitated by Western blot assay. miRs-17/20 with or without melatonin treatment suppressed the expression and activity of both the HIF1/VEGF/MMPs and the IL6R/JAK2/STAT3 axis. miRs-17/20 with or without melatonin treatment also mitigated the clinical impairment, pyknosis, and edema in the hippocampus and cortex and neurodegeneration induced by SAH. Our results show that miRs-17/20 alleviated EBI by reducing hypoxic conditions, hypoxia-induced molecular signaling, and neuronal apoptosis.

Keywords: subarachnoid hemorrhage early brain injury; microRNAs-17/20; melatonin.

1. INTRODUCTION

Subarachnoid hemorrhage (SAH) accounts for 5% of all stroke cases and emerges following the blood flow to the subarachnoid area due to rupture of arterial brain vessels. Despite encouraging treatment methods, SAH still has a poor prognosis with a 25–50% disability and mortality rate. Early brain injury (EBI) is considered a main factor of death and poor prognosis after SAH within 24–72 h [1, 2]. Thus, the prevention of EBI is one of the most important aims for the management and improvement of the acute deleterious effects of SAH [3].

Vasospasm, inflammation, oxidative stress, increased permeability of the blood–brain barrier (BBB), brain ischemia, and edema are defined as the main pathological outcomes of EBI [1, 4, 5]. Various pathways and molecules involving the EBI process have been previously demonstrated. Cerebral vasospasm has been reported to be one of the most important phenomena in EBI [6]. Interleukin-6 (IL-6) was reported as a regulator of Janus Kinase/signal transducer and activator of transcription (JAK/STAT) signaling pathway, inducing cerebral vasospasm [7]. On the other hand, the suppressor of cytokine signaling 3 (SOCs3) protein was reported as an inhibitor of JAK/STAT and IL-6 induced vasospasm [8]. The reduction of antioxidant activity and the production of excessive free radicals were suggested other remarkable consequences of EBI and vasospasm after SAH [4]. Cerebral edema has been revealed as another pathological outcome of EBI. Wang, et al. [9] clarified the causative role of hypoxia inducible factor-1-á (HIF1-á) and matrix metallopeptidase-9 (MMP9) in BBB dysfunction and cerebral edema.

[1] Faculty of Medicine, Department of Neurosurgery, Çanakkale Onsekiz Mart University, Turkey.
[2] Faculty of Medicine, Department of Medical Biology, Trakya University, Turkey.
[3] Faculty of Medicine, Department of, Physiology, Çanakkale Onsekiz Mart University, Turkey.
[4] Faculty of Medicine, Department of Histology and Embryology, İzmir Democracy University, Turkey.
[*] e-mail: umalcok@gmail.com

0091-150X/23/5706-0793 © 2023 Springer Science+Business Media, LLC

There is substantial evidence suggesting that EBI might also be closely related to the deterioration of mitochondrial function [10]. Mitochondrial dysfunction results in neuron apoptosis and autophagy [11]. Mammalian target of rapamycin (mTOR) protein is reported to be a regulator of cell autophagy and mitochondrial dysfunction related to EBI. Inhibition of mTOR with rapamycin diminishes mitochondrial fission and ameliorates neuronal injury-induced SAH via improvement of mitochondrial function [12]. The phosphatidylinositol 3-kinase/serine-threonine protein kinase (PI3K/AKT) pathway has been reported to be another pathway that has neuroprotective effects on neuronal damage owing to its antiapoptotic, antioxidative, and anti-inflammatory properties [13].

The ameliorative effects of MEL on EBI are well known and MEL was described as an adjuvant agent on EBI following SAH by antioxidant [14], antiapoptotic [15, 16] and anti-inflammatory [17] characteristics. Moreover, various molecules have also been investigated for attenuation of EBI, such as MFGE8 [18], liproxitatin-1 [19], INT-777 [20], resveratrol [21], and quercetin [22]. However, owing to the poor prognosis of EBI, rapid and easy application of supportive therapeutic methods or agents that also pass through the BBB are required for the prevention or treatment of EBI.

In recent years, microRNAs (miRs) were considered as indispensable regulators of brain pathological conditions, ranging from brain tumors to neurodegenerative diseases, implying that miRs became a novel target agent with numerous advantages for the development of therapeutic strategies [23]. miRs are 22 nucleotides noncoding RNAs, regulators of several gene expressions, and studies demonstrated that they have multiple roles in cellular processes, reflecting their effects on cell metabolism, proliferation, differentiation, apoptosis, survival, and stress response in different cell types [24]. Instability and the complex environment of miRs have become the trend of recent therapeutic approaches through their nature and unique effects. Intranasal administration of miRs can be easily applied on account of their ability to pass through the BBB [25]. miR-17 and miR-20 belong to the miRs-17/92 cluster, which participates in human chromosome 13 and the mouse chromosome 14 [26]. It was reported that miR-17 and miR-20 levels changed in spinal cord injury associated with apoptosis and miR-20 had a proinflammatory contribution, whereas miR-17 was effective on hypoxic brain injury [27–29].

Preliminary studies on the effects of miRs-17/20 and MEL and the efficiency of intranasal miR delivery convinced us to investigate the effects of both molecules on EBI after SAH. As the neuronal injury, inflammation, and vascular changes occur mostly early at 24–72 h after SAH, our study was performed within the first 24 h after SAH. We assessed the ameliorative effects of MEL and intranasal miRs-17/20 administration on EBI by evaluation of neurological scores, brain edema, oxidative stress (CuZn-SOD, Mn-SOD, CAT, and GST/M1), neuronal apoptosis (CASP3, BAX, and BCL-2), hypoxia (HIF1/VEGF/MMP9), mitochondrial dysfunction (PI3K, AKT, and mTOR), and inflammatory (IL6/JAK2/STAT3) signaling pathways. Then, the neuroprotective effects of miRs-17/20 were compared with MEL in EBI through the aforementioned molecular pathways.

2. MATERIALS AND METHODS

2.1. Animals and Experimental Design

The experimental protocols of this study were approved by the Çanakkale Onsekiz Mart University Animal Experiments Local Ethics Committee (Protocol number 2019/03-05). Male Wistar albino rats (3–4 months old weighing 250–350 g) were obtained from Çanakkale Onsekiz Mart University Experimental Research Centre. Rats were housed at 22 ± 2°C temperature and 12 h/12 h light/dark cycle. During the experiment, rats were fed with standard food pellets and water ad libitum. Rats were divided into six experimental groups with nine animals in each group, randomly assigned.

Sham group (n = 9): all stages of the SAH operation, except for blood injection to the cisterna magna, were performed. MEL and miRNA vehicles were administered at 1 h after the sham operation.

SAH group (n = 9): the SAH model was applied through the injection of 120 µl autologous arterial blood to the prechiasmatic cistern.

SAH+miRs-17/20 control group (n = 9): One hour after the SAH operation, miRs-17/20 miRNA mimic negative control#1 (200 pmol) was administered via nasal instillation.

SAH+MEL group (n = 9): the SAH model was applied and MEL (10 mg/kg) was injected intraperitoneally 1 h after SAH.

SAH-miRs-17/20 group (n = 9): mimic-miR-17 (200 pmol) and mimic-miR-20 (200 pmol) were applied via nasal instillation 1 h after SAH.

SAH+MEL+miRs-17/20 group (n = 9): both intranasal mimic-miR-17 (200 pmol) and mimic-miR-20 (200 pmol) administration and intraperitoneal MEL (10 mg/kg) injection were applied 1 h after SAH.

2.2. Anesthesia

The SAH operation was performed under general anesthesia with intramuscular ketamine hydrochloride (60–80 mg/kg) and xylazine hydrochloride (5 mg/kg). Intranasal miRNA administration was performed under isoflurane (3%) anesthesia.

2.3. MEL Preparation and Administration

The MEL (N-acetyl-5-methoxytryptamin; product code: M5250-1G; Sigma-Aldrich, St. Louis, MO, USA), was dissolved in absolute ethanol (Absolute GR for analysis, MERCK, Germany) and further dilutions were prepared in isotonic saline to reach a final concentration of 2.4% (v/v)

ethanol. MEL was administered (10 mg/kg) intraperitoneally at 1 h after SAH [30].

2.4. Intranasal miRNA Administration

The rno-miR-20b-5p mimic (miR-20) (miRBase Accession: MIMAT0003211/5 'CAAAGUGCUCAUAGUGCAGGUAG/miRVana® miRNA mimic, Thermo Scientific, USA), rno-miR-17-1-3p mimic (miR-17) (miRBase Accession: MIMAT0004710/5 'ACUGCAGUGAAGGCACUUGUGG/miRVana® miRNA mimic, Thermo Scientific, USA), and miRNAs-17/20 miRNA mimic negative control#1 (Thermo Scientific, USA) were dissolved in 10 µl of RNase-free water at 200-pmol doses for each. Rats were anesthetized with isoflurane 2% and kept in a supine position. The 10-µl solution was delivered through the right and left nares with a pipette via nasal instillation. Rats were kept under anesthesia and in a supine position for 3 min more after intranasal miR treatment [31, 32].

2.5. SAH Operation

An experimental SAH model was modified by Prunell, et al. [33] using a stereotaxic frame under general anesthesia. Briefly, the needle was tilted 30° in to the right sagittal plane and placed 7.5 mm in front of the bregma in the midline with the 1.5-mm diameter burr hole. A bone wax used to obstruct the hole in order to stop bleeding. Autologous arterial blood (120 µl), which was totally nonheparinized, was injected into the prechiasmatic cistern within 10 sec. Unlike the original model, instead of tail venous blood, arterial blood was used in our study. For the Sham group, the prechiasmatic cistern was reached by a 30G needle tip and kept on hold for 10 sec before the needle was removed.

2.6. Assessment of Mortality and Neurological Deficits

The neurological score was evaluated at 24 h after SAH, using Garcia's Neurological Scoring Scale [34]. Briefly, six tests were applied and scored as 0–3 or 1–3 and the determined scores ranged from 3 to 18. Somatic sensitivity, physical exercise, autonomic exercise, physical activity and a coordination test were applied. Severe neurological deficits were shown with low scores. Mortality rates in each group were figured out at the same time. New animals were added into the groups instead of dead rats.

2.7. Motor Coordination Tests

Static rods and horizontal rod bar tests were applied for evaluation of motor coordination abilities at the beginning of the experiment and at 24 h after SAH. Static rods consisted of four different wooden rods of varying thickness (such as 35 mm, 28 mm, 22 mm, and 15 mm). The duration access time was recorded as the animal fell or as it reached the maximum test time (120 sec). The test was stopped if the animal falls off a rod and replaced again on the rods for 5 sec for a maximum of three trials and the best results were used for evaluation.

Horizontal rod bars contained two rods with a diameter of 3 mm and 5 mm respectively. Rats were scored a full five points if they reached and touched the side bars or held on for more than 30 sec. The duration on the rod was scored as 1 point for 1–5 sec, 2 points for 6–10 sec, 3 points for 11–20 sec, and 4 points for 21–30 sec [35].

2.8. Tissue Harvesting

At the end of the study rats were sacrificed under general anesthesia and brains were harvested immediately. Afterward, brains were separated into the left and right cerebral hemispheres, hippocampus, and cerebral cortex. Six of the 9 rat brains were used for genetic and histopathological evaluation and 3 of the 9 were examined for brain water content from each group. The right hippocampus was stored at ?80°C until genetic analyses. The cerebral cortex and left hippocampus were fixed with 4% paraformaldehyde for histopathological analysis.

2.9. Brain Water Content

The brain edema was determined using the wet and dry brain weight method. Briefly, brain samples were removed immediately and weighed (wet weight) 24 h after SAH. After weighing, the brains were kept at +70°C in the oven for 72 h and weighed again (dry weight). Brain water content was calculated as [(wet weight-dry weight)/wet weight] × 100% [16].

2.10. Histopathology

Histopathological examination was preformed in the hippocampus and frontal cerebral cortex with hematoxylin and eosin (H&E) staining. The tissues were kept in neutral buffered formalin of 10% and fixed for 48 h. Following the routine steps tissues were embedded in paraffin. Then, 4-µm sections were picked up from the blocks with microtome and stained with H&E. Stained sections were examined and photographed under an Olympus CX43 camera light microscope. Tissue damage was scored as no damage: 1, mild damage: 2, moderate damage: 3, severe damage: rated over 4 points, and a dataset created both in the hippocampus and in the cerebral cortex in terms of pyknosis and interstitial edema.

2.11. Molecular Analysis

2.11.1. Chemicals and Antibodies

The MOPS buffer and NuPage gels, RIPA Lysis Buffer System, 50 ml (sc-24948) were obtained from Thermo Fisher Scientific, USA and Santa Cruz Biotechnology respectively. The PureLink® RNA Mini Kit, mirVana™ miRNA Isolation Kit, High Capacity cDNA Reverse Transcription Kit, TaqMan™ Advanced miRNA cDNA Synthesis Kit, Power SYBR® Green Master Mix, and molecular grade water were purchased from Thermo Fisher Scientific. The antibodies were HIF-1α Antibody (3C144): sc-71247;

TABLE 1. Genes and primer sequences used in quantitative real-time polymerase chain reaction

Gene ID	Name	Primer sequence (5'–3')
CuZn-SOD	Superoxide dismutase 1	**F** GGTGGGCCAAAGGATGAAGAG
		R CCACAAGCCAAACGACTTCC
Mn-SOD	Superoxide dismutase 2, mitochondrial	**F** GGAAGCCATCAAACGTGACTT
		R CCCGTTCCTTATTGAAACCAAGC
CAT	Catalase	**F** TGGAGCTGGTAACCCAGTAGG
		R CCTTTGCCTTGGAGTATTTGGTA
GST/M1	Glutathione S-transferases	**F** CCACATTTTTGAGCCCAAGT
		R TACTCCATTGGGCCAACTTC
BCL-2	B-cell CLL/lymphoma 2	**F** GGTGGGGTCATGTGTGTGG
		R CGGTTCAGGTACTCAGTCATCC
BAX	BCL2-associated X protein	**F** CCCGAGAGGTCTTTTTCCGAG
		R CCAGCCCATGATGGTTCTGAT
CASP3	Caspase-3	**F** CATGGAAGCGAATCAATGGAC
		R CTGTACCAGACCGAGATGTCA
HIF-1α	Hypoxia-inducible factors-	**F** AGCCAGATCTCGGCGAAGT
	1α	**R** CAGAGGCCTTATCAAGATGCG
HIF-1β	Hypoxia-inducible factors-1β	**F** CAAGCCCCTTGAGAAGTCAG
		R GAGGGGCTAGGCCACTATTC
VEGF	Vascular endothelial growth factor	**F** AGGAGGGCAGAATCATCACG
		R CAAGGCCCACAGGGATTTTCT
VEGFR	Vascular endothelial growth factor receptor	**F** TGAAGGAAGGCAGATCGTCAT
		R CAGGTTATTCGCTTCCCATCA
MMP3	Matrix metallopeptidase 3	**F** AGTCTTCCAATCCTACTGTTGCT
		R TCCCCGTCACCTCCAATCC
MMP9	Matrix metallopeptidase 9	**F** TACCCTATGTACCGCTTCAC
		R GAACAAATACAGCTGGTTCC
IL-6	Interleukin 6	**F** ATGAACTCCTTCTCCA CAAG
		R AGAGCCCTCAGGCT GGACTG
IL-6R	Interleukin 6 receptor	**F** CAGCTGAGAACGAGGTGTCC
		R GCAGCTTCCACGTCTTCTTGA
JAK2	Janus Kinase 2	**F** CAGTGGTCAAGAGGGAAACA
		R TGTCTGAGCGAACAGTTTCC
SOCs3	Suppressor of Cytokine Signalling-3	**F** GCTCCAAAAGCGAGTACCAGC
		R AGTAGAATCCGCTCTCCTGCAG
SOCs7	Suppressor of Cytokine Signalling-7	**F** CAGGCCCTGAATTACCTC
		R ACTGAACCTGACCGTACAGAGGTTGCTGCT GCTGCT
STAT3	Signal Transducer And Activator Of Transcription 3	**F** GGAGGAGTTGCAGCAAAAAG
		R TGTGTTTGTGCCCAGAATGT
PI3K	Phosphatidylinositol 3-kinase	**F** CCTGATCTTCCTCGTGCTGCTC
		R ATGCCAATGGACAGTGTTCCTCTT
AKT	Serine/Threonine Protein Kinase	**F** TTGTCATGGAGTACGCCAACG
		R ACAGCCCGAAGTCTGTGATCTT

TABLE 1. Continued

Gene ID	Name	Primer sequence (5'–3')
mTOR	Mechanistic Target Of Rapamycin Kinase	**F** GGCCGACTCAGTAGCAT
		R CGGGCACTCTGCTCTTT
rno-miR-20b-5p	MIMAT0003211	**F** GCAAAGTGCTCATAGTGCAG
		R GGTCCAGTTTTTTTTTTTTTTTCTAC
rno-miR-17 – 1 – 3p	MIMAT0004710	**F** CTGCAGTGAAGGCACTT
		R TCCAGTTTTTTTTTTTTTTCCACA
PCR conditions	1 cycle of 2 min at 50°C and 10 min at 95°C followed by 40 cycles of denaturation at 95°C for 15 sec, annealing and extension at 60°C for 1 min	

VEGF Antibody (JH121): sc-57496 (Santa Cruz, USA); JAK2 Monoclonal Antibody (691R5), Phospho-JAK2 [p Tyr1007, p Tyr1008] antibody (SY24 – 03), STAT3 (232209) antibody, Phospho-STAT3 (Tyr705) Antibody (710093) (Thermo Fisher Scientific), Actin Monoclonal Antibody (ACTN05 (C4)), (Thermo Fisher Scientific), and secondary horseradish peroxidase-linked anti-mouse and anti-rabbit IgG antibodies supplied by WesternBreeze™ Chemiluminescent Kit, antimouse and antirabbit (Thermo Fisher, Scientific).

2.11.2. RNA and miRNA Isolation, Reverse Transcription, and qRT-PCR Assay

Total RNA was isolated from the hippocampus of each group (five replicates) using a Purelink RNA purification kit (Thermo Fisher Scientific, USA). The cDNAs were synthesized using a High-Capacity cDNA Reverse Transcription Kit (Thermo Fisher Scientific, USA). qRT-PCR analysis was performed on a Quant studio 5 real-time PCR (Life Technologies, USA) using the Power Syber Green Gene Expression Master Mix (Life Technologies, USA). The thermal cycling condition and oligonucleotide primer sequences are explained in Table 1. Relative expression levels of mRNA and miRNA were calculated by the comparative cycle threshold ($2^{-\Delta\Delta Ct}$) method and the ribosomal RNA 18S for mRNA and U47 for miRNA used as endogen control [36].

2.12. Immunoblot Analysis

Hippocampus samples were homogenized three times for 5-min periods with Daihan 15D high speed homogenizator (27,000 rpm) in 500 µl RIPA lysis buffer combining 2 µl PMSF solution, 2 µl sodium orthovanadate solution, and 2 µl protease inhibitor cocktail solution (RIPA Lysis Buffer System, sc-24948, Santa Cruz, USA) under ice cold conditions. Homogenate was centrifuged at 14,000×*g* for 20 min and approximately 0.67–1.36 mg/mL total protein was determined by the Protein A280 method in a microvolume spectrophotometer (Optizen Nano Q, Mecasys, Korea). After denaturation, proteins were loaded onto a NuPAGE® Bis-Tris polyacrylamide gel (10%), electrophoresed, and transferred to PVDF membranes (Life Technologies, USA). The membranes were incubated in 5% milk in TBS buffer. Antibodies were diluted according to band intensity in antibody binding buffer overnight under dark room conditions (+4°C) and then incubated in the secondary antibody solution containing antimouse IgG-HRP and antirabbit IgG-HRP for 1 h. Washed and enhanced immunoblots, protein bands were observed with a chemiluminescence Micro ChemiDoc, (DNR Bio-Imaging Systems Ltd, USA) gel imaging system. Bands were quantified by GelQuant software.

2.13. Statistical Analyses

Six independent groups were compared according to clinical and histological datasets. Nonparametric tests were used for distribution of non-normal data. Kruskal–Wallis test was used for comparison between groups. The significance was inferred at p?0.05. The differences in gene expression levels between control and experimental groups were determined by one-way ANOVA, Tukey HSD test. Both statistical analyses were performed using SPSS 20 software. Data were presented as mean ± standard error (SE). Fold change data for gene expression was calculated using the $2^{-\Delta\Delta Ct}$ method.

3. RESULTS

3.1. Mortality and SAH Operation

The number of rats that died within 24 h following SAH were recorded as 6, 4, 4, 3, 3 in the SAH, SAH+miRs-17/20 control, SAH+MEL, SAH+miRs-17/20+MEL, and SAH+miRs-17/20 groups respectively. None of the sham-operated rats died. Although severe hemorrhage after SAH was observed in the subarachnoid area of the SAH and SAH+miRs-17/20 control groups, reduced hemorrhage was observed both in MEL and miRs-17/20 administered groups. Representative images of hemorrhage accumulated in the subarachnoid spaces of the brain are presented in Fig. 1.

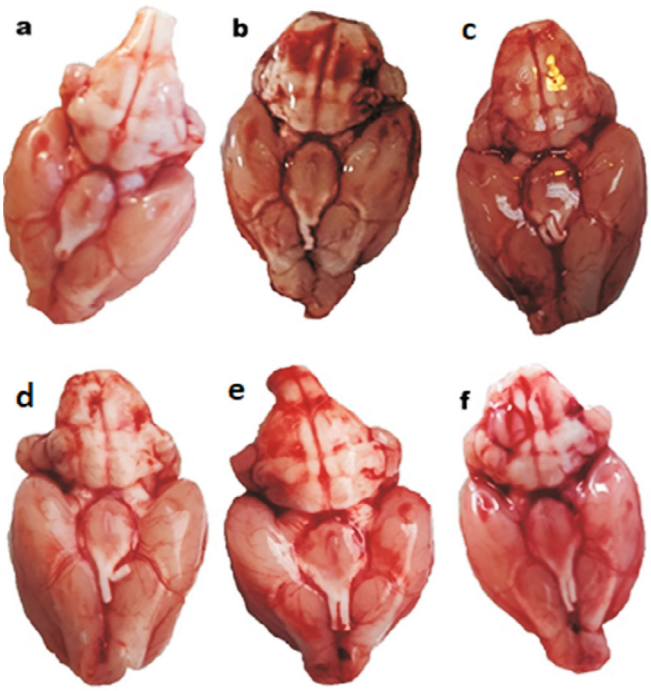


Fig. 1. Photographs represent hemorrhage of the subarachnoid area. **a**, **b**, **c**, **d**, **e**, and **f** indicated Sham, SAH, SAH+miRs-17/20 control, SAH+MEL, SAH+miRs17-20, and SAH+MEL+miRs-17/20 groups, respectively.

3.2. Brain Water Content Results

Although the administration of MEL and miRs-17/20 decreased edema in the brain according to histopathological evaluation, there was no statistically significant difference in brain water content outcomes (Table 2) ($p > 0.05$).

3.3. Neurological Evaluation

Neurological deficits were evaluated using Garcia's Neurological Scoring Scale, static rods, and horizontal rod bars tests. All evaluation applied before and at the 24th hour after SAH or the Sham operation.

3.3.1. Garcia's Neurological Scoring Scale

All rats received 18 full points for the evaluation of Garcia's Neurological Scoring Scale before the experiment. At the 24th hour after the SAH, all groups were able to maintain their Garcia score. Although there were differences between the groups in Garcia scores, the differences were not statistically significant (Table 2; $p > 0.05$).

3.3.2. Static Rod Test

The total time of the rats to complete the tests on 4 different diameter static rods were summed up, the differences between the averages before and after the experiment were compared. The positive increase in the average time indicates that the motor and coordination skills deteriorated. It was observed that SAH+miRs-17/20 group scores were close to those of the Sham. There were significant differences between the SAH and SAH+miRs-17/20 control compared with the Sham (Table 2; $p < 0.001$). The better motor skills were observed in the miRs-17/20 group compared with the MEL group (Table 2; $p < 0.001$).

3.3.3. Horizontal Rod Bars Test

The motor skills of the SAH group were significantly impaired compared with the SAH+MEL+miRs-17/20 and SAH+miRs-17/20 groups (Table 2; $p < 0.05$).

Static rod and horizontal rod bars tests indicate that motor coordination skills deteriorated after SAH; however, both MEL and miRs-17/20 administration have revealed ameliorative effects. Moreover, the ameliorative effects of miRs-17/20 were more potent than those of MEL.

3.4. Histopathological Evaluation

Determination of the effects of MEL and miRs-17/20 on pyknosis, interstitial edema, and apoptosis, H&E staining was performed on the frontal cortex and hippocampus. Representative images of pyknosis and interstitial edema are presented in Fig. 2.

TABLE 2. The total Garcia score, static rod duration and horizontal bar duration, and brain water content values

Evaluation method	Garcia score (score)	Static rods (s)	Horizontal bars (s)	Brain water content (%)
Sham	18 ± 0	48 ± 17	0.6 ± 0.2	74.56
SAH	16 ± 0.6	285 ± 62*	2.8 ± 0.3*	74.50
SAH+miRs-17/20 control control	16 ± 0.6	240 ± 41*	2.7 ± 0.4*	75.32
SAH+MEL	17 ± 0.8	159 ± 37**	1.9 ± 0.6	75.15
SAH+miRs-17/20	17 ± 0.5	54 ± 27 ×	0.9 ± 0.4**	74.89
SAH+MEL+miRs-17/20	17 ± 0.5	116 ± 51	1.6 ± 0.9**	74.99

Compared with Sham *$p < 0.01$, **$p < 0.05$, compared with SAH *** $p < 0.01$ for static rod results. Compared with Sham * $p < 0.001$ and compared with SAH **$p < 0.01$ for horizontal bar results. Values are expressed as mean ± SE of mean.

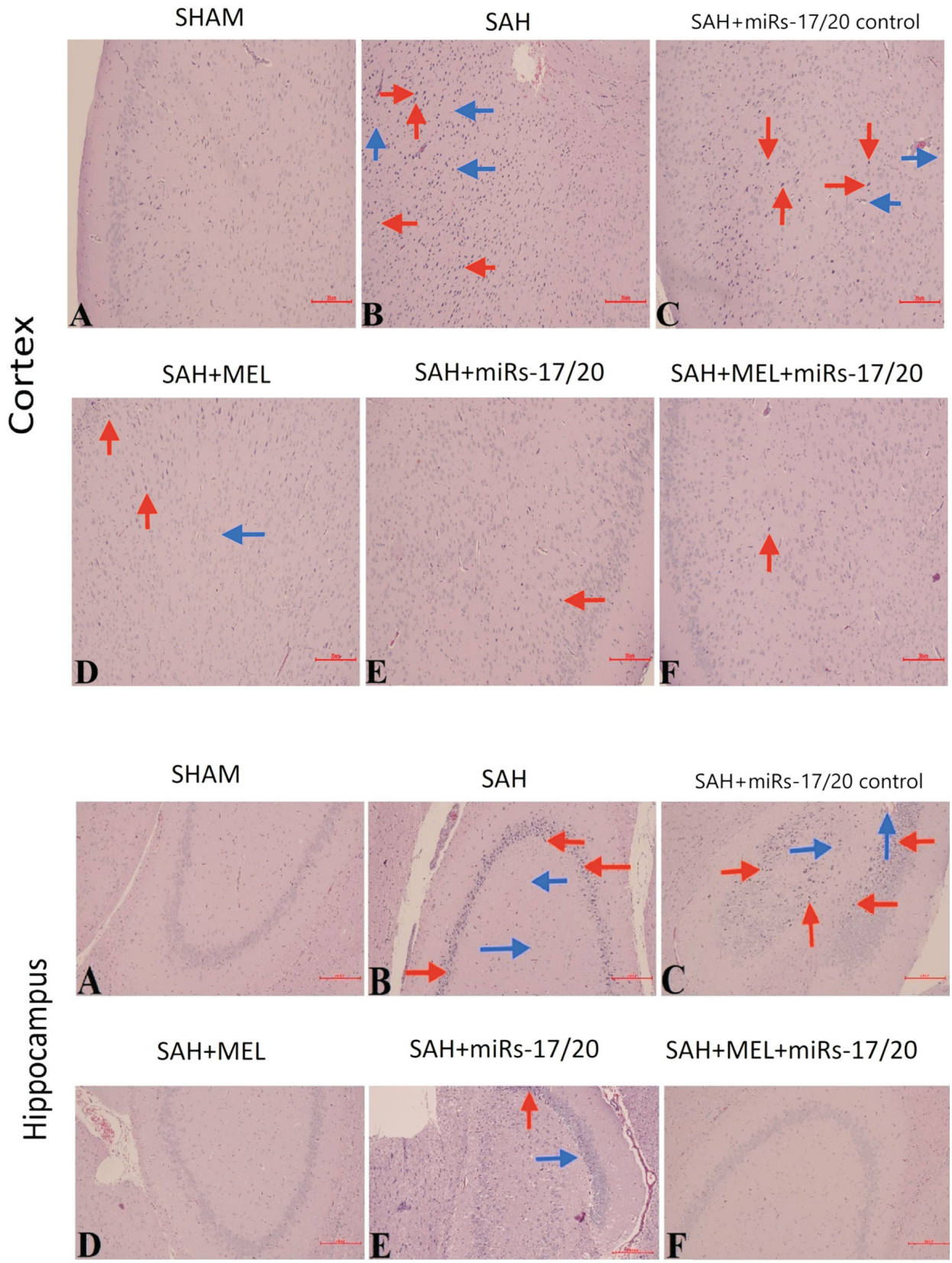


Fig. 2. Hematoxylin and eosin-stained cortex and hippocampus images of histological slices of the experiment groups. **A**, **B**, **C**, **D**, **E**, and **F** belong to Sham, SAH, SAH+miRs-17/20 control, SAH+MEL, SAH+miRs17-20, and SAH+MEL+miRs-17/20 groups respectively. Pyknosis is represented by red and interstitial edema by blue arrows (magnification ×100).

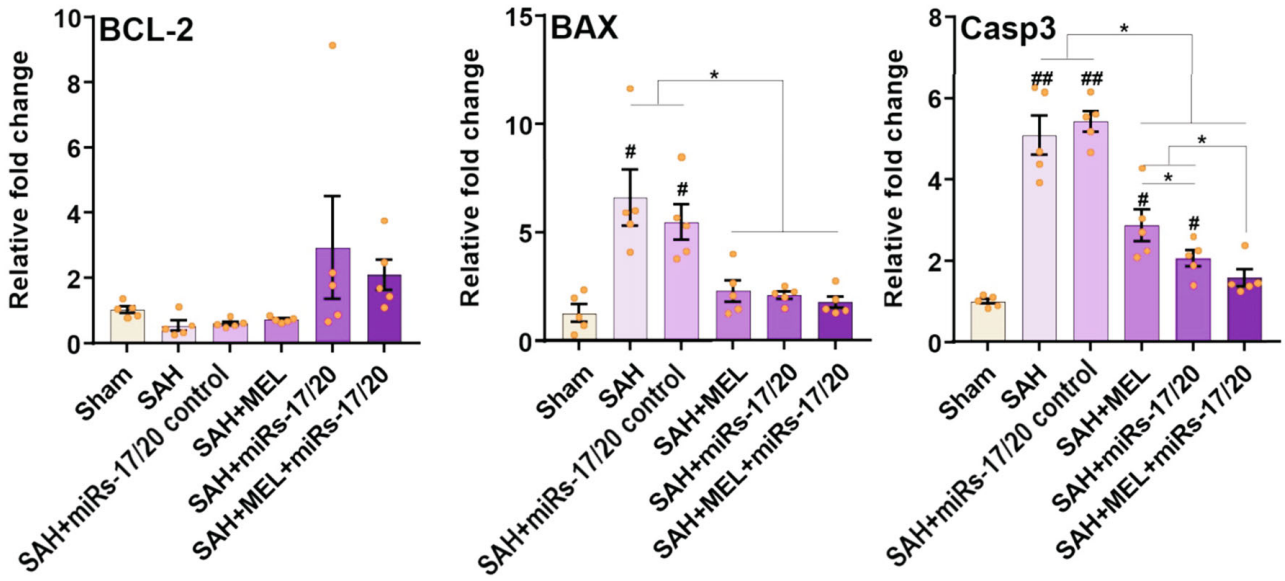


Fig. 3. Relative fold change was determined by quantitative real-time polymer chain reaction analysis of BCL-2, BAX, and Caspase 3 genes in the hippocampus of the Sham and experimental groups. All data were normalized with 18S expression and given as relative to control; data were represented as mean ±SD. $^{\#}p \le 0.05$, $^{\#\#}p \le 0.01$ Sham *vs* other experimental groups, $^{*}p \le 0.05$ indicates significantly different value, analyzed by one-way ANOVA, Tukey test. Sham: Sham operated, SAH: Subarachnoid hemorrhage, SAH+miRs-17/20 control: treated with degenerate-miRNAs, SAH+MEL: treated MEL, SAH+miRs-17/20: treated with miRs-17/20, SAH+MEL+miRs-17/20: treated with miRs-17/20 and MEL.

It was determined that there was no statistically significant difference between the Sham, SAH+MEL, and SAH+MEL+miRs-17/20 groups according to total pyknosis scores of brain cortex (Table 3; $p > 0.05$). However, it was observed that the pyknosis scores of these three groups were significantly decreased compared with the SAH and SAH+miRs-17/20 control groups (Table 3; $p < 0.001$). Moreover, significantly increased pyknosis scores were observed in hippocampus of the SAH and SAH+miRs-17/20 control groups (Table 3; $p < 0.001$). Similar pyknosis scores were obtained in the Sham and SAH+MEL+miRs-17/20 groups (Table 3; $p > 0.05$). These results indicate that both MEL and miRs-17/20 treatment produced moderate ameliorative effects on pyknosis in hippocampus and cerebral cortex.

Significantly increased edema scores were obtained in the SAH group compared with Sham in both hippocampus and cortex cerebri (Table 3 and Fig. 2; $p < 0.05$). We also observed moderate ameliorative effects on edema in both MEL and miRs-17/20 treatment groups.

The values shown as superscript characters are different from other values in the same line ($p < 0.05$). Values are expressed as total scores. Kruskal–Wallis tests were applied and $p < 0.05$ value was accepted as statistically significant.

3.5. Apoptosis-Related Gene Expression

Further, we investigated the transcription levels of BCL-2, BAX and Caspase-3 as markers of mitochondrial apoptosis. BCL-2 gene expression levels decreased in the SAH and SAH+-miRs-17/20 control groups but statistically insignificantly (Fig. 3; $p > 0.05$). However, a significant increase in BAX and Caspase-3 gene expression levels was observed in both SAH and SAH+miRs-17/20 control groups compared with the others (Fig. 3; $p < 0.05$ or $p < 0.01$). These results indicate that MEL and miRs-17/20 have a strong ameliorative effect on SAH-induced EBI via inhibiting apoptosis.

TABLE 3. Hematoxylin and eosin (H&E) staining results

Evaluation method		Brain area	Sham	SAH	SAH+miRs-17/20 control	SAH+MEL	SAH+miRs-17/20	SAH+MEL+miRs-17/20
H&E staining and total scores	Interstitial edema	Hippocampus	6^{a}	18^{b}	15^{b}	15^{b}	14^{b}	12^{b}
		Cortex	6^{a}	17^{b}	10^{a}	$12^{b, c}$	$10^{a, c}$	$8^{a, c}$
	Pyknosis	Hippocampus, 8^{a}	$20^{b, c}$	15^{b}	$17^{b, c}$	$13^{a, c}$	$15^{b, c}$	
		Cortex, 9^{a}	22^{b}	15^{c}	$14^{a, b}$	15^{b}	$14^{a, b}$	

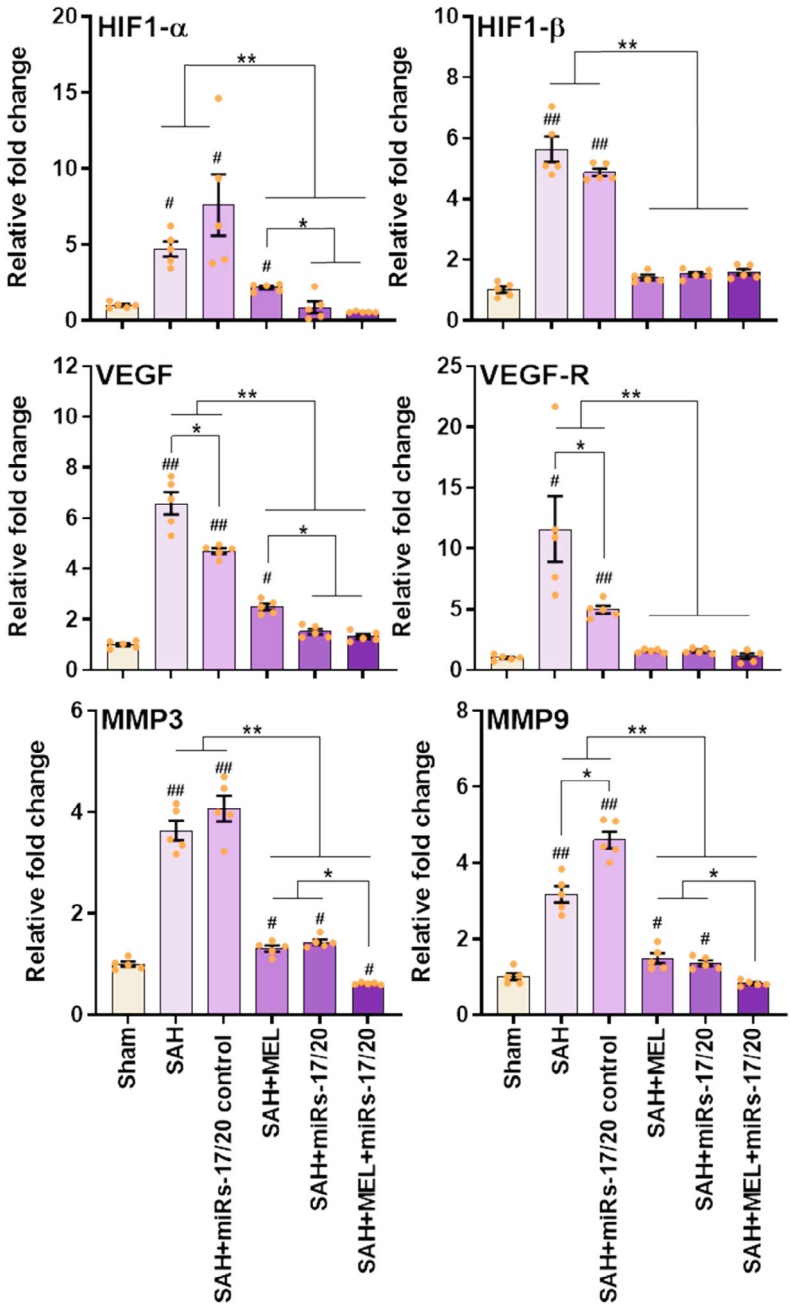


Fig. 4. Relative fold change determined by quantitative real-time polymer chain reaction analysis of hypoxia-/angiogenesis-related genes in the Sham and experimental groups of hippocampus. All data were normalized with 18S expression and given as relative to control; data were represented mean ± SD. $^{\#}p \leq 0.05$, $^{\#\#}p \leq 0.01$ Sham *vs* other experimental groups. $^{*}p \leq 0.05$; $^{**}p \leq 0.01$ indicates a significantly different value, analyzed by one-way ANOVA, Tukey test. Sham: Sham operated, SAH: Subarachnoid hemorrhage, SAH+miRs-17/20 control: treated with degenerate-miRNAs, SAH+MEL: treated MEL, SAH+miRs-17/20: treated with miRNAs-17/20, SAH+MEL+miRs-17/20: treated both miRNAs-17/20 and MEL.

3.6. Hypoxia/Angiogenesis-Related Gene Expression

Gene expression related to hypoxia and angiogenesis markers HIF1-α, HIF1-β, VEGF, VEGF-R, MMP3, and MMP9 was significantly increased in the SAH group compared with the Sham, SAH+MEL, SAH+miRs-17/20, and SAH+MEL+miRs-17/20 groups (Fig. 4; $p < 0.001$). There was no significant difference between the SAH and SAH+miRs-17/20 control group (Fig. 4; $p > 0.05$).

3.7. IL-6/JAK2/STAT3 Pathway-Related Gene Expression

We examined JAK2, STAT3, SOCS3, SOCS7, IL-6, and interleukin-6 receptor gene expression levels to determine

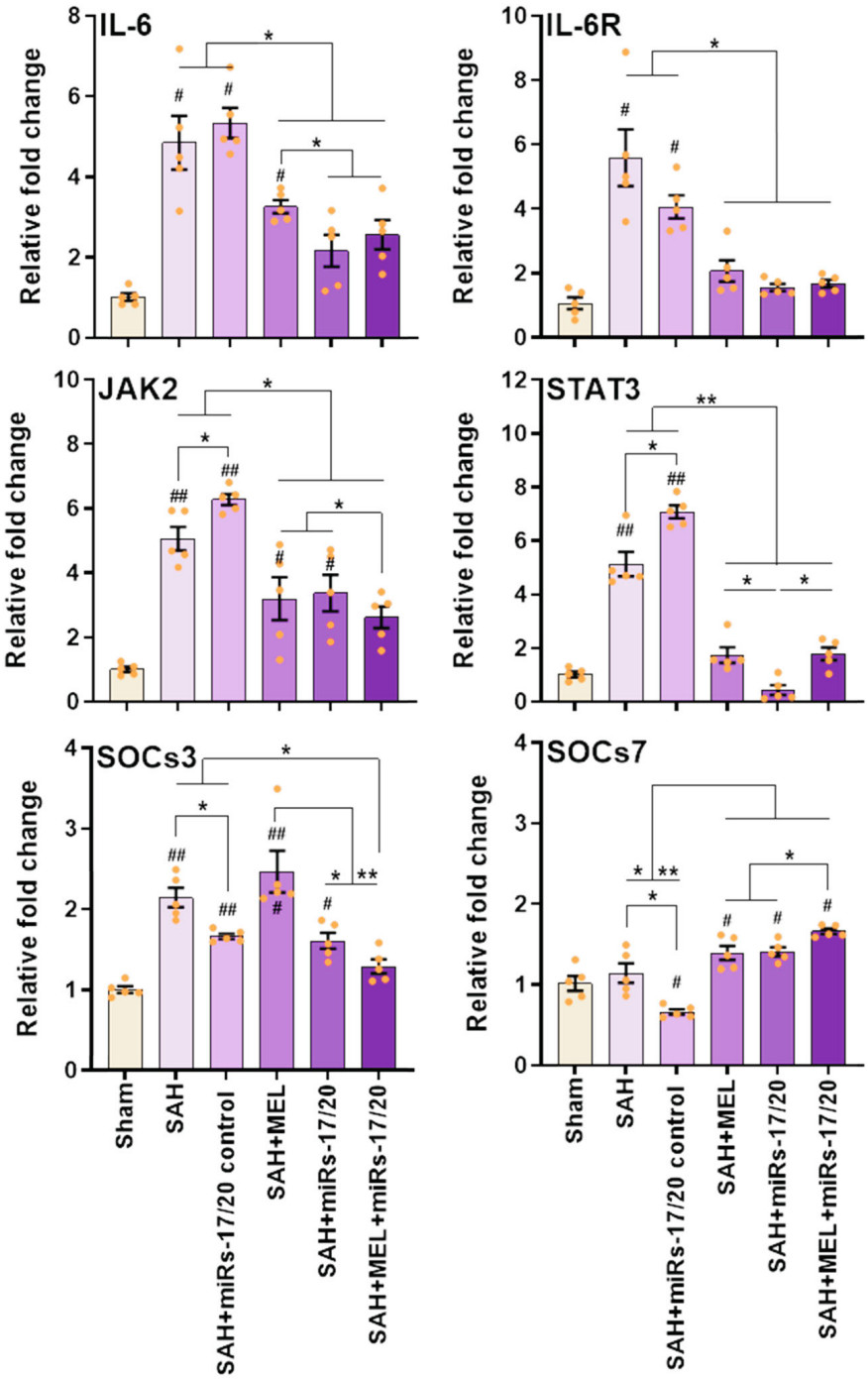


Fig. 5. Relative fold change determined by quantitative real-time PCR (qRT-PCR) analysis of IL-6 receptor-dependent JAK/STAT signals genes in the Sham operated and experimental groups of hippocampus. All data were normalized with 18S expression and given as relative to control; data were represented mean ± SD. $^{\#}p \leq 0.05$, $^{\#\#}p \leq 0.01$ Sham vs other experimental groups. $^{*}p \leq 0.05$; $^{**}p \leq 0.01$ indicates significantly different values, analyzed by one-way ANOVA, Tukey test. Sham: Sham operated, SAH: Subarachnoid hemorrhage, SAH+miRs-17/20 control: treated with Degenerate-miRNAs, SAH+MEL: treated with MEL, SAH+miRs-17/20: treated with miRNAs-7/20, SAH+MEL+miRs-17/20: treated both miRNAs-17/20 and MEL.

the effects of MEL and intranasal miR-17/20 administration (Fig. 5). IL-6 and IL-6R gene expressions levels were increased in SAH and SAH+miRs-17/20 control groups compared with others (Fig. 5; $p < 0.05$). Further, the higher JAK2 and STAT3 gene expression levels were also obtained in SAH and SAH+miRs-17/20 control groups (Fig. 5;

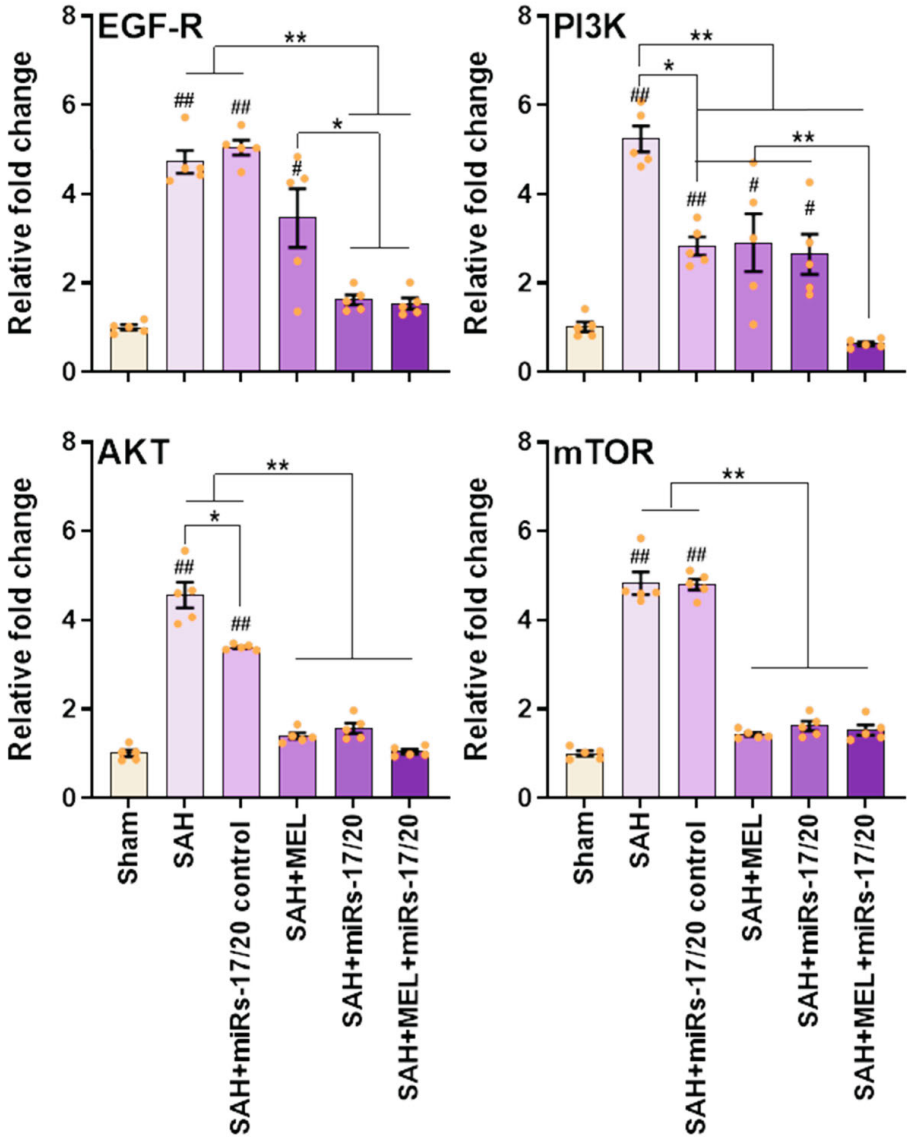


Fig. 6. Relative fold change determined by quantitative real-time polymer chain reaction analysis of EGFR and PI3K/AKT/mTOR signaling genes in the Sham operated control and experimental groups of hippocampal tissue of rats. All data were normalized with 18S expression and given as relative to control; data were represented as mean ± SD. $^{\#}p \leq 0.05$, $^{\#\#}p \leq 0.01$ Sham vs other experimental groups $^{*}p \leq 0.05$; $^{**}p \leq 0.01$ indicates a significantly different value, analyzed by one-way ANOVA, Tukey test. Sham: Sham operated, SAH: Subarachnoid hemorrhage, SAH+miRs-17/20 control: treated with Degenerate-miRNAs, SAH+MEL: treated MEL, SAH+miRs-17/20: treated with miRNAs-17/20, SAH+MEL+miRs-17/20: treated with miRNAs-17/20 and MEL.

$p < 0.01$). These outcomes indicate that MEL and miRs-17/20 have potent anti-inflammatory effects through inhibition of the IL-6/JAK2/STAT3 pathway.

There was no significant difference between the Sham and SAH+MEL+miRs-17/20 group in terms of SOCs3 expression level (Fig. 5; $p > 0.05$). We observed that MEL and miRs-17/20 administration caused SOCs7 gene expression (Fig. 5; $p < 0.05$). The data revealed that contrary to the changes of IL-6, JAK2, and STAT3 expression, the alterations of SOCs3 and SOCs7 expression were not significant in our study.

3.8. PI3K/AKT/mTOR Pathway Gene Expression

The expression levels of EGF-R, AKT, PI3K, and mTOR genes in charge of the PI3K/AKT/mTOR pathway was also examined, which mediates many cellular processes such as cell survival, proliferation, migration, and autophagy. SAH operation increased EGF-R gene expression levels. Administration of miRs-17/20 and MEL decreased EGF-R gene expression levels (Fig. 6; vs SAH and SAH+miRs-17/20 control ($p < 0.01$). The significant decrease in the PI3K/AKT/mTOR pathway was observed in the co-treat-

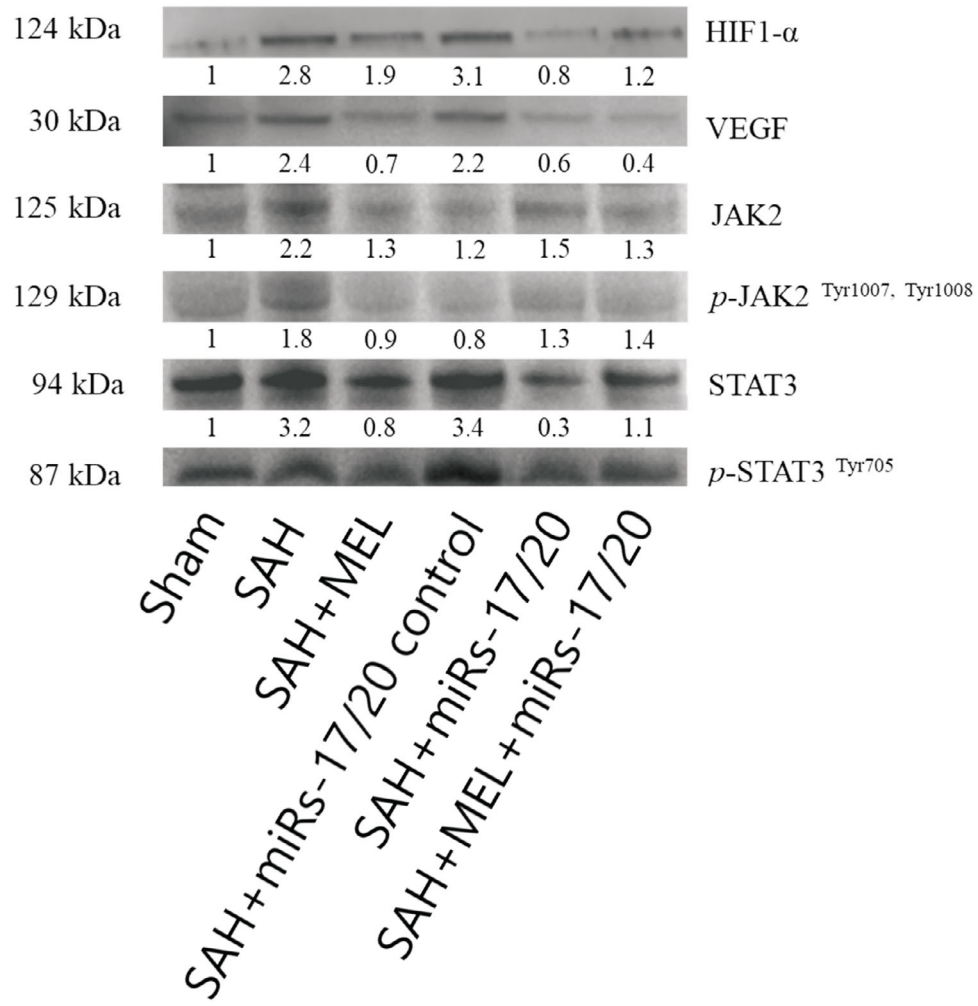


Fig. 7. Immunoblot band distribution of HIF1-α, VEGF, JAK2, p-JAK2Tyr1007, Tyr1007, STAT3, and p-STAT3Tyr705 proteins.

ment of MEL- and miRs-17/20-administered groups compared with SAH (Fig. 6; $p < 0.05$ or $p < 0.01$).

3.9. Immunoblot Analysis

In our study, immunoblot was performed for HIF1-α, VEGF, JAK2, *p*-JAK2$^{Tyr1007,\ Tyr1007}$, STAT3, and *p*-STAT3^{Tyr705} protein expressions (Fig. 7).

4. DISCUSSION

To our knowledge this study is the first report to demonstrate that intranasal miRs-17/20 administration alleviates EBI thorough regulation of the edema and hypoxia (HIF1-α, HIF1β, VEGF, VEGFR-R, MMP3, and MMP9), apoptosis- and neuronal injury-related proteins (PI3K, AKT, and mTOR), and the inflammatory pathway (JAK2, STAT3, IL-6, IL-6R, and SOCs7).

Extensive hemorrhage commonly occurs at the Willis polygon after SAH in humans. We preferred to study the prechiasmatic cistern SAH model. In our study, SAH was induced by injection of nonheparinized autologous artery blood to the prechiasmatic cistern modified from Prunnel, et al. [33]. We obviously observed hemorrhage in brain samples (Fig. 1). On the other hand, we also obtained apoptosis, pyknosis, and interstitial edema of histopathological evaluation of hippocampus and frontal cortex as a sign of neuronal injury (Fig. 2). We also experienced that neurological scores (except for Garcia scores) deteriorated significantly in the SAH group. Macroscopic and microscopic findings and neurological evaluation revealed that our experimental SAH model is appropriate and efficient for investigating SAH-induced EBI.

It is known that hypoxia commonly occurs after SAH [37]. Also, it has been determined that VEGF levels increase in brain with hypoxia [38]. On the other hand, VEGF administration in cerebral microcirculation leads to an increase in BBB permeability and dilatation in the cerebral arterioles [39]. HIF1-α and HIF1-β, two endogenous signal proteins, are commonly triggered by ischemia and hypoxia, and both

of them are tightly related with brain disorders [40]. It has been reported that HIF1-α, HIF1-β, and VEGF gene expression levels increase within 24 h after SAH accompanied by disruption of the BBB and cerebral edema [41]. Furthermore, Wang, et al. [10] determined that both HIF1-α and MMP9 gene expression levels increased after SAH. In that study, it was also observed that HIF1-α and MMP9 levels decreased after treatment with selective inhibitors. In accordance with previous studies, it was observed that HIF1-α, HIF1β, MMP3, and MMP9 levels increased within 24 h of SAH in our study. Moreover, significant increases were identified in VEGF and VEGF-R levels in the SAH group and miRs-17/20 treatment reduced HIF1-α, HIF1-β, MMP3, MMP9, VEGF, and VEGF-R gene expression levels (Fig. 4). For all these parameters significant reductions were also determined in MEL-administered groups. However, when all the parameters were evaluated together, it was observed that the strongest effect occurred in the co-treatment of MEL and miRs-17/20. It has been reported that inhibition of HIF1-α in an acute period after SAH has neuroprotective effects [42, 43]. HIF1-α has also been characterized as a key molecule reducing brain edema after SAH as it has reducing effects on MMP9 gene expression levels [10]. In our study, both MEL and miRs-17/20 administration reduced the brain edema-associated gene expression levels of the above-mentioned molecules. HIF1-α is a key molecule for oxygen homeostasis. It has been reported that, the miR17/92 cluster regulated HIF1-α expression in lung cancer cells [44]. Ma, et al. (2016) showed that angiogenesis-inducing factors such as transforming growth factor β type II receptor (TGFBR2), VEGF, and HIF1-α are inhibited by miR17/92 both in vivo and in vitro [45]. Moreover, the inhibitory effect of miR-20b on HIF1-α and VEGF levels was reported [46]. miRNAs are small noncoding RNAs that act as regulators of post-transcriptional gene expression and binds on specific targets of mRNAs for cleavage or downregulation [47]. In our study the downregulation of HIF1-α and VEGF gene expressions took the source from the aforementioned features of miRNAs.

Many studies consistently reported that apoptosis and necrosis commonly occur following SAH. As reducing apoptosis and increasing autophagy play an important role in the prevention of EBI after SAH we investigated apoptosis-related gene expression levels on behalf of the PI3K/AKT/mTOR pathway. We determined that the administration of MEL and miRs-17/20 suppressed gene expression related to the PI3K/AKT/mTOR pathway (Fig. 6). mTOR functions as a serine/threonine kinase acting in basic biological processes, and controls cell survival, the cell cycle, cell differentiation, and migration [48]. Previous studies clarified that the PI3K/AKT/mTOR signaling pathway mediates autophagy and apoptosis in the central nervous system [49]. Lin, et al. reported the reduction in the mTOR pathway and brain damage of a traumatic injury model with the administration of MEL sourced from the decrease in inflammation and the induction of autophagy process. It was determined that MEL strongly suppressed mTOR activity in traumatic brain injury in rats suggesting that the suppression of mTOR might be a mechanism of the protective effects of MEL against inflammatory response and apoptosis in brain injuries [50]. In parallel to previous results about the effects of MEL on SAH-induced apoptosis, our results demonstrated that MEL also strongly suppressed mTOR (Fig. 6). Furthermore, this is the first study to reveal the effects of intranasal miRs-17/20 administration on SAH-induced apoptosis in hippocampus and cerebral cortex. It has been previously demonstrated that miR-20 has anti-apoptotic effects on spinal damage [51]. Chen, et al. [27] previously demonstrated that activation of IRE1α, by degenerating miR-17 – 5p, stabilized TXNIP mRNA and increased TXNIP levels to activate NLRP3 inflammasome and amplify brain injury. In addition, it has been found that miR-17 could inhibit hypoxia-induced apoptosis in kidney and heart [52, 53]. Wang, et al. [54] reported that resveratrol alleviated lipopolysaccharide-induced injury in a human keratinocyte cell line through activations of the PTEN/PI3K/AKT and mTOR pathways, which were modulated by miR-17. However, there is no previous finding on the use of intranasal miRs-17/20 treatment in SAH and effects on SAH-induced apoptosis. Our data demonstrated for the first time that intranasal miRs-17/20 treatment after SAH strongly suppressed the mTOR, increased the Bcl-2, and decreased BAX gene expression levels (Fig. 5). Consequently, we suggest that intranasal miRs-17/20 treatment, on its own, could alleviate SAH-induced apoptosis in the brain as powerfully as MEL.

The JAK2/STAT3 pathway was also evaluated in our study to determine the effects of MEL and miRNAs-17/20 on EBI after SAH through an inflammatory pathway (Fig. 5). The JAK2/STAT3 pathway includes the JAK and STAT families and JAK proteins are activated by the binding of cytokines to their specific receptors. Activated JAKs also activate STAT protein, which regulates expression of a number of genes. There are limited and incompatible data, not only on JAK2/STAT3 signaling for gene regulation in the central nervous system but also JAK2/STAT3 change in the brain after SAH and the relationship with MEL. In addition, to the best of our knowledge, the therapeutic effects of intranasal miRs-17/20 treatment on the JAK2/STAT3 pathway in SAH have not yet been studied. IL-6 is a proinflammatory cytokine that activates the JAK2/STAT3 signaling pathway and transduces signals to the nucleus from the cell surface [55]. SOCS proteins work together with the catalytic domains of JAK2 proteins and inhibit JAK2 kinase activity, cause a decrease in STAT3 activity [56]. The SOCS3 gene expression immediately increases in response to activation of IL-6 and inhibits signal transduction of IL-6 [57]. Thus, we evaluated both IL-6 and SOCS together with the JAK2/STAT3 pathway. The SOCS protein plays an impor-

tant role in the inhibition of the JAK2/STAT3 signaling pathway [58]. Lili, et al. [58] reported that pre-treatment with propofol attenuated hippocampal injury via the JAK2/STAT3 pathway stimulated by autogenously orthotropic liver transplantation. Furthermore, Xun and Zheng [59] notified that there is a relationship among pain, inflammation, and inflammatory cytokines in a model of experimental neuropathic pain in rats and declared that dexmedetomidine administration has protective effects through downregulation of pro-inflammatory cytokines and inhibits the JAK2/STAT3 pathway. In our study, it was observed that IL-6 and IL-6R gene expressions were increased. Moreover, JAK2/STAT3 gene expressions and protein levels increased after SAH. MEL and miRs-17/20 treatment revealed a significant reduction in JAK2, STAT3, IL-6, and IL-6R gene expression. These results indicate that the JAK2/STAT3 pathway became active in SAH groups, and MEL and miRs-17/20 administration strongly suppressed this activation (Fig. 5). According to our results, it can be suggested that one of the suppressive effects of MEL and miRs-17/20 on the JAK2/STAT3 pathway is the stimulation of SOCS7 (Fig. 5).

The relationship between microRNA and inflammation has drawn attention, and the miR17/92 cluster and inflammatory relationship with cancer development are continuing to be investigated. One of miR17/92 cluster host gene members, miR17HG gene, encodes more than six mature miRNAs, which are miR-17, miR-18a, miR-19a, miR-19b, miR-20, and miR-92 [60]. A novel study performed with rats in a rheumatoid arthritis model showed that miR17 suppressed both IL-6 and the JAK-STAT pathway [61]. Besides anti-inflammatory effects of miR17, there are various reports on the anti-inflammatory effects of miR20b too; on the other hand, some studies reported that miR20b promotes the inflammation [28, 62]. miR20b is also asserted as a suppressor of STAT3 gene expression in the liver by the binding site of the miR20b GCAAUCUGGGCACUUU sequence as a signal transducer and (STAT)3 3'-untranslated region. After the transfer of miR-20b mimics into H22 cells, the STAT3 is downregulated [63]. Our results claimed that the inflammation was suppressed after SAH in hippocampus and reduced JAK2/STAT3 gene expression levels. These findings clarified that in our study the mixture of miRNA had a totally anti-inflammatory effect.

miRs are tiny noncoding RNAs that are made up of around 20–25 nucleotides, act in regulation of the expression of several target genes through sequence-specific hybridization to the 3' untranslated region of messenger RNAs. miRs either completely inhibit the translation, or directly deteriorate to target miRs and play irreplaceable roles in multiple biological pathways, including metabolic control, immune modulation, cell cycle, neuronal development, stem cell differentiation, and muscle differentiation [64].

The prevention of EBI is considered to be one of the most important aims of the reduction of acute effects and management of SAH. Hence, SAH-induced EBI treatment requires further studies that target supportive new agents that are effective and easily diffuse through the BBB. Most of the agents that are used in SAH treatment have limited BBB permeability, require high doses, and involve several adverse effects. In recent years, miRNA therapy has been a promising target for neurodegenerative diseases. However, orally administered mimic miRNAs have short half-lives and also require high doses in order to cross the BBB [65]. For this reason, intranasal drug administration such as nose-to-brain miRNA therapy has been considered an alternative method for treatment of brain diseases. This method offers a direct bypass of the BBB, allows high intracerebral doses to be reached, and has few adverse effects [31]. As miRNAs reach the brain cells, cell-penetrating peptides function as potential vectors for delivering miRNA into the cell [66]. Mai, et al. [31] demonstrated an 8.0-fold peak at 30 min and a 1.75-fold peak at 24 h M146AG levels in hippocampus after intranasal miR146a administration in mice. In another study, 12 hours after intranasal miR132 treatment, a higher miR132 level was observed in hippocampus [32]. Thus, for miR17-20 administration we used the intranasal route and the aforementioned results suggested to us that sufficient and effective miR17-20 could reach the hippocampus following nose-to-brain miRNA administration after 1 h after SAH in our study.

In our study, we considered that intranasal miRNA therapy could be one supportive treatment of EBI. In recent years, it was determined that some miRNA levels have changed many diseases, suggesting that miRs could be a potential agent in medical treatment. It has already been demonstrated that the levels of miR-17 and miR-20 change in spinal cord injury (SCI). It has been stated that miR-20 is effective in the proinflammatory process and that miR-20 is downregulated and miR17 is upregulated after SCI [28]. In another SCI study, miR-17 and miR-20 have been associated with anti-apoptotic properties [29]. However, to the best of our knowledge, there is a lack of information about the effects of intranasal miR-17 and miR-20 administration on SAH. This is the first study aimed at explaining the effectiveness of both miRs in SAH-induced EBI through investigation of edema, hypoxia, apoptosis, neural injury, and inflammatory-related proteins. Recently, studies clarified that the intranasal administration of miRs has protective effects on brain diseases [31]. Moreover, Samaridou, et al. [32] emphasized that a nose-to-brain delivery system could be a reliable and effective way of transitioning medicines in brain diseases. Our results notified that adequate miRs-17/20 reached the brain after intranasal administration and have a decreasing effect on brain edema, hypoxia, and injury, similar to MEL. For instance, miR-17 and miR-20 reduced EGF-R, PI3K, HIF1-α, and MMP3 levels after SAH compared with the MEL group.

5. CONCLUSION

Our results revealed that MEL and/or miRs-17/20 administration have significantly alleviated EBI following SAH, reducing pyknosis and brain edema, and also improving neurological scores. Both miRs-17/20 and MEL have also had inhibitory effects on apoptosis, hypoxia-related injury, and inflammation. Our findings support the hypothesis that MEL and miRs-17/20 administration directly target hypoxia and apoptosis pathways. Furthermore, our findings suggest that MEL and miRs-17/20 may have therapeutic value in the treatment of EBI through its targeting of the key molecular signals of the brain.

ETHICAL APPROVAL

This study was approved by the Ethics Committee of Çanakkale Onsekiz Mart University, Turkey. (Decision number 2019/03-05).

ACKNOWLEDGMENT

This work was funded by the Scientific Research Coordination Unit (BAPD) of Çanakkale Onsekiz Mart University, Çanakkale, Turkey (Project Number: TSA-2019-2943).

CONFLICTS OF INTEREST STATEMENT

The authors declare that there are no conflicts of interest.

DATA AVAILABILITY

Data will be made available on request; also, data that have been used are confidential.

REFERENCES

1. V. Friedrich, R. Flores and F. A. Sehba, *Neurosci. Lett*., **512**(1), 6–11 (2012).
2. V. Rass and R. Helbok, *Front. Aging Neurosci*., **19**(10), 78 (2019).
3. M. Gaasch, A. J. Schiefecker, M. Kofler, et al., *Crit. Care Med.*, **46**(5), 774 – 780 (2018).
4. R. E. Ayer and J. H. Zhang, *Acta Neurochir. Suppl*., **104**, 33 – 41 (2008).
5. F. A. Sehba, J. Hou, R. M. Pluta, et al., *Prog. Neurobiol*., **97**(1), 14 – 37 (2012).
6. J. L. Leclerc, J. M. Garcia, M. A. Diller, et al., *Front. Mol. Neurosci*., **11**(71) (2018).
7. K. Osuka, Y. Watanabe, K. Yamauchi, et al., *Brain Res. J*., **1072**(1), 1 – 7 (2006).
8. K. Osuka, N. Usuda, M. Aoyama, et al., *Neurosci. Lett.,* **21**(569), 55 – 58 (2014).
9. Z. Wang, C. J. Meng, X. M. Shen, et al., *J. Mol. Neurosci.*, **48**(1), 273 – 280 (2012)
10. Z. Wang, X. Y. Shi, J. Yin, et al., *J. Mol. Neurosci*., **46**(1) (2012).
11. C. H. Jing, L. Wang, P. P. Liu, et al., *Neuroscience*, **213**, 144 – 53 (2012).
12. Y. Li, P. Wu, J. Dai, et al., *Cell. Mol. Neurobiol*., **40**(4), 629 – 642 (2020).
13. C. Y. Zhang, X. M. Ren, H. B. Li, et al., *Eur. Rev. Med. Pharmacol. Sci*., **23**(11), 4890 – 4897 (2019).
14. F. Deghan, M. Khaksari Hadad, G. Asadikram, et al., *Arch. Med. Res*., **44**(4), 251 – 258 (2013).
15. J. Chen, L. Wang, C. Wu, et al., *J. Pineal Res*., **56**, 12 – 19 (2014).
16. K. Ding, J. Xu, H. Wang, et al., *Neurochem. Int.,* **91**, 46 – 54 (2015).
17. M. C. Tsai, W. J. Chen, M. S. Tsai, et al., *J. Pineal Res*., **51**(2), 233 – 245 (2011).
18. J. Wang, Y. Wang, Y. Zuo, et al., *Exp. Brain Res.*, **239**, 2193–2205 (2021).
19. Y. Cao, Y. Li, C. He, et al., *Neurosci. Bull.*, **37**(4), 535 – 549 (2021).
20. X. Hu, J. Yan, L. Huang, et al., *Brain Behav. Immun.*, **91**, 587 – 600 (2021).
21. D. Guo, J. Xie, J. Zhao, et al., *NeuroReport*, **29**(5), 368 – 379 (2018).
22. Ş. Gül, E. Aydoğmuş, B. Bahadir, et al., *Turk. J. Med. Sci*., **50**(4), 1106 – 1110 (2020).
23. H. Sabaie, N. Amirinejad, M. R. Asad, et al., *Front. Aging Neurosci*., **25**(13), 742242 (2021).
24. N. Shekari, M. Asadi, M. Akbari, et al., *Eur. Rev. Med. Pharmacol. Sci.*, **26**(4), 1268 – 1282 (2022).
25. C. Zhou, P. Sun, Y. Xu, et al., *Adv. Sci.*, **11**, e2104986 (2022).
26. E. Mogilyansky and I. Rigoutsos, *Cell Death Differ.*, **20**(12), 1603 – 1614 (2013).
27. D. Chen, B. J. Dixon, D. M. Doycheva, et al., *J. Neuroinflammation*, **15**(32) (2018).
28. M. Nieto-Diaz, F. J. Esteban, D. Reigada, et al., *Front. Cell. Neurosci*., **8**(53) (2014).
29. N. K. Liu, X. F. Wang, Q. B. Lu, et al., *Exp. Neurol*., **219**(2), 424 – 429 (2009).
30. M. Uzun, M. Gencer, H. Turkon, et al., *Arch. Med. Res.*, **48**(7), 592 – 598 (2017).
31. H. Mai, F. Weihao, W. Yan, et al., *Mol. Ther. - Nucleic Acids*, **18**, 681 – 695 (2019).
32. E. Samaridou, H. Walgrave, E. Salta, et al., *Biomaterials*, **230**, 119657 (2020).
33. G. F. Prunell, T. Mathiesen and N. A. Svendgaard, *NeuroReport*, **13**(18), 2553 – 2556 (2002).
34. J. H. Garcia, S. Wagner, K. F. Liu, et al., *Stroke*, **26**(4), 627 – 634 (1995).
35. R. M. Deacon, *J. Vis. Exp*., **29**(75), 2609 (2013).
36. H. Kang and A. Hata, *Curr. Opin. Hematol*., **19**(3), 224 – 231 (2012).
37. K. E. Wartenberg and S. A. Mayer, *Neurosurg. Clin. N. Am*., **21**(2), 325 – 338 (2010).
38. D. Saraswat, S. Nehra and K. Chaudhary, *Clin. Exp. Pharmacol. Physiol*., **42**(5), 475 – 484 (2015).
39. W. G. Mayhan, *Am. J. Physiol*., **276**(5), C1148 – 1153 (1999).
40. G. L. Wang, B. H. Jiang, E. A. Rue, et al., *Proc. Natl. Acad. Sci. USA*, **92**(12), 5510 – 5514 (1995).
41. C. Wu, Q. Hu, J. Chen, et al., *Biochem. Biophys. Res. Commun*., **437**(3), 469 – 744 (2013).
42. O. Baranova, L. F. Miranda, P. Pichiule, et al., *J. Neurosci*., **27**(23), 6320 – 6332 (2007).
43. W. Chen, V. Jadhav, J. Tang, et al., *Neurobiol. Dis*., **31**(3), 433 – 441 (2008).
44. A. Taguchi, K. Yanagisawa, M. Tanaka, et al., *Cancer Res*., 68(14), 5540–5545 (2008).
45. H. Ma, J. S. Pan, L. X. Jin, et al., *Cancer Lett*., **376**(2), 293 – 302 (2016).

46. Z. Lei, B. Li, Z. Yang, et al., *PLoS One*, **4**(10), e7622009 (2009).
47. J. Brennecke, A. Stark, R. B. Russell, et al., *PLoS Biology*, **3**(3), e85 (2005).
48. C. G. Proud, *Biochem. Soc. Trans*., **35**(5), 1187 – 1190 (2007).
49. T. Ersahin, N. Tuncbag and R. Cetin-Atalay, *Mol. Biosyst*., **11**(7), 1946 – 1954 (2015).
50. C. Lin, H. Chao, Z. Li, et al., *J. Pineal Res*., **61**(2), 177 – 186 (2016).
51. X. J. Liu, X. P. Zheng, R. Zhang, et al., *Int. J. Clin. Exp. Pathol*., **8**(4), 3811 – 3818 (2015).
52. M. Zhou, J. Cai, Y. Tang, et al., *Med. Hypotheses*, **81**(1), 108 – 110 (2013).
53. T. Kaucsár, C. Révész, M. Godó, et al., *Nucleic Acid Ther*., **23**(5), 344 – 354 (2013).
54. X. Wang and Y. Zhang, *Biochem. Biophys. Res. Commun*., **2**(598), 141 (2022).
55. P. C. Heinrich, I. Behrmann, S. Haan, et al., *Biochem. J*., **374**(1), 1 – 20 (2003).
56. H. Yasukawa, *EMBO J.,* **18**(5),1309 – 2130 (1999).
57. R. Starr, T. A. Willson, E. M. Viney, et al*., Nature*, **387**, 917–921(1997).
58. J. Lili, W. Fe, G. Xiangqian, et al., *Brain Res.*, **15**(1657), 202 – 207 (2017).
59. S. Xun and R. Zheng, *J. Cell Biochem*., **121**(3), 2277 – 2283 (2020).
60. C. S. Fuziwara and E. T. Kimura, *Front. Med.*, **2**, 64 (2015).
61. A. Najm, F. M. Masson, P. Preuss, et al., *Arthritis & Rheumatol.*, **72**, 12. (2020).
62. Z. Liu, H. Yu and Q. Guo, *Mol. Med. Rep.*, **17**, 1 (2018).
63. Y. Luo, J. He, X. Tao, et al., *Oncol. Rep.*, **40**, 5 (2018).
64. A. F. Christopher, R. P. Kaur, G. Kaur, et al., *Perspect. Clin. Res*., **7**(2), 68 – 74 (2016).
65. W. G. Mayhan, *Am. J. Physiol*., **276**(5), C1148 – 1153 (1999).
66. Y. Zhang, M. Köllmer, J. S. Buhrman, et al., *Peptides*, **58**, 83 – 90 (2014).